Cryovolcanic features on Titan's surface as revealed by the Cassini Titan Radar Mapper

R.M.C. Lopes [a,*], K.L. Mitchell [a], E.R. Stofan [b], J.I. Lunine [c,r], R. Lorenz [c], F. Paganelli [a], R.L. Kirk [d], C.A. Wood [e], S.D. Wall [a], L.E. Robshaw [f], A.D. Fortes [g], C.D. Neish [c], J. Radebaugh [c], E. Reffet [c], S.J. Ostro [a], C. Elachi [a], M.D. Allison [h], Y. Anderson [a], R. Boehmer [a], G. Boubin [c], P. Callahan [a], P. Encrenaz [i], E. Flamini [j], G. Francescetti [k], Y. Gim [a], G. Hamilton [a], S. Hensley [a], M.A. Janssen [a], W.T.K. Johnson [a], K. Kelleher [a], D.O. Muhleman [l], G. Ori [m], R. Orosei [n], G. Picardi [o], F. Posa [p], L.E. Roth [a], R. Seu [o], S. Shaffer [a], L.A. Soderblom [d], B. Stiles [a], S. Vetrella [k], R.D. West [a], L. Wye [q], H.A. Zebker [q]

[a] *Jet Propulsion Laboratory, California Institute of Technology, Pasadena, CA 91109, USA*
[b] *Proxemy Research, Bowie, MD 20715, USA*
[c] *Lunar and Planetary Laboratory, University of Arizona, Tucson, AZ 85721, USA*
[d] *US Geological Survey, Flagstaff, AZ 86001, USA*
[e] *Wheeling Jesuit University, Wheeling, WV 26003, USA*
[f] *Environmental Sciences Department, Lancaster University, Lancaster LA1 4YQ, UK*
[g] *Department of Earth Sciences, University College London, London WC1E 6BT, UK*
[h] *Goddard Institute for Space Studies, National Aeronautics and Space Administration, New York, NY 10025, USA*
[i] *Observatoire de Paris, 92195 Meudon, France*
[j] *Agenzia Spaziale Italiana, 00131 Rome, Italy*
[k] *Facoltá di Ingegneria, 80125 Naples, Italy*
[l] *Division of Geological and Planetary Sciences, California Institute of Technology, Pasadena, CA 91125, USA*
[m] *IRSPS, Pescara, Italy*
[n] *CNR-IASF, 00133 Rome, Italy*
[o] *Universitá La Sapienza, 00184 Rome, Italy*
[p] *INFM and Dip. Interateneo di Fisica, Politecnico di Bari, 70126 Bari, Italy*
[q] *Stanford University, Stanford, CA 94305, USA*
[r] *INAF-IFSI, 00133 Rome, Italy*

Abstract

The Cassini Titan Radar Mapper obtained Synthetic Aperture Radar images of Titan's surface during four fly-bys during the mission's first year. These images show that Titan's surface is very complex geologically, showing evidence of major planetary geologic processes, including cryovolcanism. This paper discusses the variety of cryovolcanic features identified from SAR images, their possible origin, and their geologic context. The features which we identify as cryovolcanic in origin include a large (180 km diameter) volcanic construct (dome or shield), several extensive flows, and three calderas which appear to be the source of flows. The composition of the cryomagma on Titan is still unknown, but constraints on rheological properties can be estimated using flow thickness. Rheological properties of one flow were estimated and appear inconsistent with ammonia–water slurries, and possibly more consistent with ammonia–water–methanol slurries. The extent of cryovolcanism on Titan is still not known, as only a small fraction of the surface has been imaged at sufficient resolution. Energetic considerations suggest that cryovolcanism may have been a dominant process in the resurfacing of Titan.

---

* Corresponding author.
 E-mail address: rosaly.m.lopes@jpl.nasa.gov (R.M.C. Lopes).

1. Introduction

The Cassini Titan Radar Mapper (Elachi et al., 2005a) obtained Synthetic Aperture Radar (SAR) images of Titan's surface during four of the spacecraft's targeted fly-bys of Titan (Fig. 1). These fly-bys occurred on October 26, 2004 (referred to as Ta), on February 15, 2005 (T3), on September 7, 2005 (T7), and October 28, 2005 (T8). The images obtained using SAR revealed that Titan is very complex geologically (Elachi et al., 2005a, 2005b). One of the geologic processes shaping Titan's surface features is likely cryovolcanism (ice-rich volcanism). Cryovolcanic eruptions are eruptions of icy-cold aqueous or nonpolar molecular solutions or partly crystallized slurries, derived by partial melting of ice-bearing materials (Kargel, 1995). Several features that appear to be the results of cryovolcanic eruptions were identified in Ta, including a possible volcanic dome, three craters that appear to be of volcanic origin, and extensive flows. No features that could be as clearly interpreted as cryovolcanic were identified in the three other fly-bys (T3, T7, and T8), though several likely cryovolcanic features were identified in the T3 and T8 fly-bys. In this paper we discuss possible cryovolcanic features identified in the SAR images, their local geological context, possible analogs on Earth and other planets, and preliminary results on the rheology of cryolavas on Titan, which give clues to their composition.

Cryovolcanism on Titan had been proposed long before Cassini (e.g., Lorenz, 1996). Titan is sufficiently large that, during accretion, much of the body may have melted. Its interior could still contain a substantial layer of water or water–ammonia liquid (e.g., Stevenson, 1992; Grasset and Sotin, 1996; Grasset et al., 2000; Tobie et al., 2005; Mitri and Showman, 2005). Thermal convection can occur in the stagnant lid regime in Titan's ice I shell (McKinnon, 2006; Mitri and Showman, 2005; Mitri et al., 2006), floating on an ammonia–water ocean (Grasset and Sotin, 1996; Grasset et al., 2000; Tobie et al., 2005; Mitri et al., 2006). Mitri et al. (2006) showed that ammonia–water mixtures can erupt from a subsurface ocean on Titan through the ice shell, leading to cryovolcanism. They proposed that cryovolcanism is probably related to bottom crevasse formation in an ice shell floating on an ammonia–water ocean, transport of ammonia–water pockets to the base of the stagnant lid by convective motions in the ice, and refreezing of chambers of ammonia–water. Mitri et al. (2006) also argued that, rather than steady-state volcanism over the history of the Solar System, cryovolcanism on Titan could have been associated with a late onset of convection is a cooling shell.

Cryovolcanic features have been detected on other outer planet satellites (e.g., Kargel, 1995; Prockter, 2004). The possibility of finding cryovolcanic features on Titan had been discussed (e.g., Lorenz, 1993, 1996), including the prediction that resulting features were expected to be different from those on other satellites such as Triton, since the presence of a thick atmosphere on Titan will suppress the vesiculation of bubbles in a cryomagma, reducing the distribution of explosive products, and will speed the cooling of cryolavas (Lorenz, 1993). Cryomagma composition is likely primarily a mixture of water ice and ammonia, possibly with some methanol (Kargel, 1995; Kargel et al., 1991; Lorenz, 1996), although alternative compositions have been suggested, such as ammonium sulfates (Fortes and Grinrod, 2006a). According to Lorenz (1996), cryovolcanic eruptions on Titan, either present day or in the past, are more likely effusive than explosive, as a result of both the high atmospheric pressure and the relatively volatile-poor magma compositions ($<1\%$ methane) that are predicted. Recently, however, Grindrod and Fortes (2006) have modeled explosive cryovolcanism driven by the decomposition of entrained methane hydrate xenoliths.

The SAR swath shows evidence of effusive cryovolcanic features which are discussed here (see also Elachi et al., 2005b), but so far no features have been identified that appear to have resulted from explosive eruptions (such as plume deposits or steep-sided volcanic edifices). We note, however, that in some cases it can be difficult to distinguish effusive from explosive products (e.g., lava flows versus pyroclastic flows) even in terrestrial remote sensing images.

On Titan, cryovolcanism may be an important resurfacing process and a major contributor to atmospheric methane (CH_4). Since methane is photo-dissociated in Titan's atmosphere and forms ethane (Yung et al., 1984), the replenishment of methane is thought to be accomplished by means of either large bodies of surface liquids (not found so far) or from an internal reservoir, by cryovolcanism. The Gas Chromatograph Mass Spectrometer (GCMS) instrument on board the Huygens probe detected the radiogenic isotope of Argon 40 in Titan's atmosphere (Niemann et al., 2005). This isotope is a product of potassium 40 decay (half life $\sim$1.2 Gyr) and its presence, at a concentration of $\sim$43 ppm, requires that the atmosphere must be in communication with a reservoir of the parent atom. Titan is large enough to have differentiated, so it is likely that most of the potassium-bearing material is silicate rocks forming Titan's core, with perhaps a small amount leached out into solution in ice or a subsurface water–ammonia ocean (e.g., Tobie et al., 2005). Cryovolcanism would be one means by which this material might be brought to the surface.

Some observational support for the existence of cryovolcanism has also been reported. Roe et al. (2005) reported that clouds outside the south polar region form almost exclusively near 40° S, and the clustering of clouds was reported at 350° W, leading to the suggestion that they may be related to geysers or volcanic eruption of methane from the icy interior. Sotin et al. (2005) proposed that a feature from Cassini's Visible and Infrared Mapping Spectrometer (VIMS) might be cryovolcanic in origin, and suggested that the upwelling of large cryovolcanic plumes may be releasing sufficient methane into the atmosphere
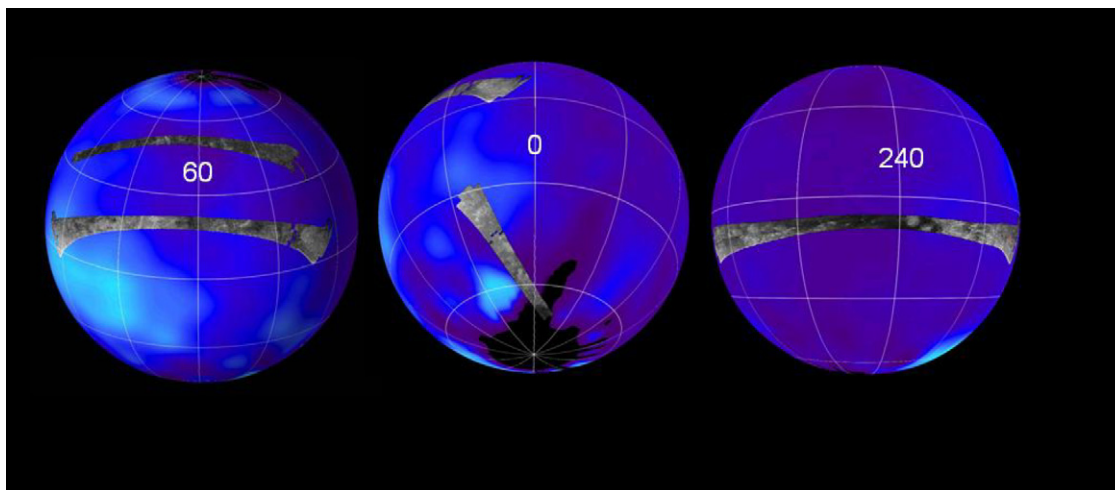
Fig. 1. The first four SAR swaths obtained by the Cassini Radar Mapper are superimposed on a false-color image made from observations by NASA's Hubble Space Telescope. Central longitudes are marked. Left: The northernmost swath is from the Ta fly-by (October 26, 2004), the lower swath is from the T3 (February 15, 2005) fly-by. Middle: The eastern end of the T3 swath is shown, as well as the T7 swath, obtained on September 7, 2005. Right: Near-equatorial swath obtained during the T8 fly-by (28 October 2005).

to account for the known atmospheric composition. Fortes and Grindrod (2006b) proposed the possibility of mud volcanoes on Titan and tentatively suggested that some dark features in one of the radar images taken during the T3 fly-by could be volcanic edifices.

2. Cassini Titan Radar Mapper observations and fly-by geometry

Cassini carries a multimode Ku-band (13.78 GHz, $\lambda = 2.17$ cm) radar instrument (Elachi et al., 2005b, 2005c) designed to probe the surface of Titan and that of other targets in the Saturn system in four operating modes—imaging, altimetry, scatterometry, and radiometry. An overview of Titan results using all four modes is given by Elachi et al. (2005b). The SAR mode is used at altitudes under ∼4000 km, resulting in spatial resolution ranging from ∼350 m to >1 km. Images are acquired either left or right of nadir using 2–7 looks. A swath 120–450 km wide is created from 5 antenna beams. SAR coverage is dependent on spacecraft range and orbital geometry. Radar backscatter variations in SAR images can be interpreted in terms of variations of surface slope, near-surface roughness, or near-surface dielectric properties. On Titan, the likely surface materials (water ice, water–ammonia ice and other ice mixtures, hydrocarbons, tholins) are different from those of bodies previously imaged with planetary radars, and volume scattering may be significant (Elachi et al., 2005b, 2005c).

The SAR mode was used in the Ta, T3, T7, and T8 fly-bys (Fig. 1). The SAR strip obtained during Ta extended from 133° W, 32° N and continued through closest approach (at a range of 1174 km) to 12° W, 29° N. The total area covered by SAR in Ta was 0.9×10^6 km^2. The SAR coverage for T3 was larger (1.8×10^6 km^2) and at lower latitudes (centered at ∼30° N and 70° W) and overlapped, for the first time, with coverage by the optical remote sensing instruments aboard Cassini, such as ISS and VIMS. The T7 swath was at high southern latitudes, centered at ∼12° W and 51° S (covering approximately

0.5×10^6 km^2), while T8 was equatorial and extended from 7° N to 18° S latitude and 179° W to 320° W longitude, covering approximately 1.79×10^6 km^2. Spatial resolution for all swaths ranged from about 350 m/pixel to 1.5 km/pixel. Preliminary results from the Ta and T3 fly-bys were discussed by (Elachi et al., 2005b, 2005c).

The SAR swaths revealed a wide variety of geologic features, including radar-bright flows, a circular volcanic construct, channels, dune-like deposits, and radar-smooth terrains that are candidates for liquids. There is plentiful morphological evidence that liquids have flowed on Titan (Elachi et al., 2005b, 2005c; Tomasko et al., 2005; Lorenz et al., in preparation), but it is not easy to differentiate between the processes that created the flow-like morphologies. Possibilities include both cryovolcanism and fluvial processes. While several features interpreted as likely cryovolcanic were identified in the Ta swath, and numerous tentatively identified on the T8 swath, there were no features on T7 that were as confidently identified as cryovolcanic in origin, and only some tentative interpretations of cryovolcanic flows on T3 were made (Elachi et al., 2005c).

3. Cryovolcanic features from the Ta fly-by

3.1. Ganesa Macula

The most prominent feature in the SAR Ta strip is a large circular feature about 180 km in diameter, seen almost in its entirety, centered at approximately 49.7° N, 87.3° W (Figs. 2B and 3). This feature was named Ganesa Macula (a macula is a dark, sometimes irregular spot on a planetary surface) and is interpreted as a volcanic edifice, either a dome (Elachi et al., 2005b) or a shield volcano. The feature (Fig. 3) is radar-bright at the edges, particularly on the instrument facing (southern) slopes, consistent with the shading that would be seen on a positive relief feature with steep sides and a relatively flat top, similar to the pancake domes on Venus imaged by Magellan [see

Fig. 2. SAR swath obtained during the Ta fly-by on October 26, 2004. Cryovolcanic features were identified in the areas marked and are discussed in detail in the text. (A) Western crater and flow. (B) Ganesa Macula and associated flows. (C) Large flow complex. (D) Eastern crater and flow.
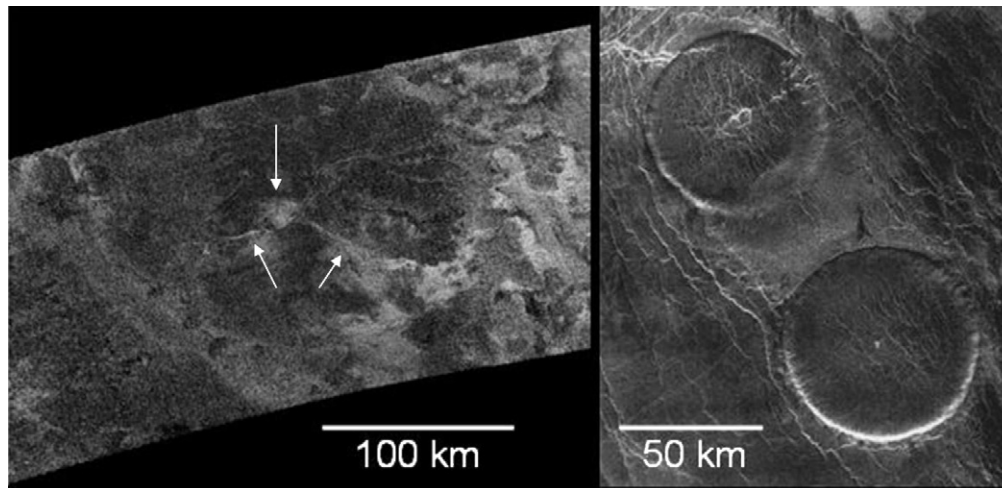

Fig. 3. Titan's Ganesa Macula (left), which we interpret as a cryovolcanic dome or shield, compared with steep-sided ("pancake") domes on Venus imaged by Magellan (NASA press release image PIA00084). Ganesa's central caldera and two channels on the flanks are indicated by arrows. The Magellan image has been rotated (north is to the left) so that the radar illumination is similar to Cassini's (from the bottom of images). See Fig. 4 for the local context for Ganesa.

descriptions by Pavri et al. (1992) and Crumpler et al. (1997)]. Ganesa has an apparent central depression about 20 km in diameter which we interpret as a volcanic pit crater or caldera. The central part of the edifice is radar dark except for a few patches of bright, lobate materials interpreted as flows (Fig. 4).

At least four sinuous channels or ridges can be seen meandering from the central crater to the edges, which are possibly cryolava channels running down the flanks of the volcanic feature. An alternative interpretation is that they could be erosional channels carved by liquid methane, or low-viscosity ammonia hydrates, emplaced after the edifice formed. One possibility is that cracks developed as cryolavas cooled, and methane from rain later collected in the cracks, which became predefined pathways for pluvial and fluvial activity. Channels on the edifice are located mostly on the eastern and southern sides (Figs. 3 and 4). Flow features that appear to have erupted from the dome are also preferentially located on the south and eastern sides, and flow features near Ganesa are all to the east of the dome. Flow directions are consistently toward the east and southeast, implying a regional gradient (Fig. 4c).

One of the sinuous channels on the southern flank can be traced for 91 km and opens out into a boot-shaped area that may be a depression, from where a radar-bright flow emanates (unit Gf in Fig. 4c). This would be consistent with the interpretation that the sinuous channel is a cryolava channel and possible source of the flow. This radar-bright flow is one of at least two distinct flows that can be mapped on Ganesa (Fig. 4c). Both appear to be connected (and maybe originate from) channels

on the southern and eastern flanks of the edifice. The southern flow is at least 75 km in length, possibly much longer, as it flows beyond the boundary of the radar swath. The area of the part imaged by radar is at least 2180 km^2. The eastern flow is at least 85 km in length, and at least 840 km^2 in area. These are minimum values as it is not possible to map the flow beyond this length, as the region immediately east of Ganesa is very complex, with many overlapping flows (Figs. 4a and 4b). These flows are comparable in length and area with volcanic flows on Mars (for example, Alba Patera; Lopes and Kilburn, 1990) and Venus (e.g., Roberts et al., 1992; Magee and Head, 2001).

Ganesa Macula (Fig. 3) has morphological similarities to pancake or steep-sided domes on Venus imaged by Magellan (McKenzie et al., 1992). The Titan feature is significantly larger in diameter (∼180 km) than the Venus domes (mean diameter ∼20 km, Fink et al., 1993), but like the Venus domes it is circular, radar dark in the central part, shows a central depression and channels or cracks on top and flanks. However, so far we have no conclusive evidence that Ganesa's central part is flat or that it has steeply sloping sides, although it appears so from a qualitative perspective (the radar illumination in Fig. 3 is from the south). Steep-sided domes were predicted to form on Titan. Lorenz (1996) argued that water–ammonia cryomagmas would probably have <1% of methane as volatile—not enough at Titan's atmospheric pressure to produce explosive eruptions. Given the high viscosity of water–ammonia mixtures (e.g., Kargel, 1995), Lorenz and Mitton (2002) proposed
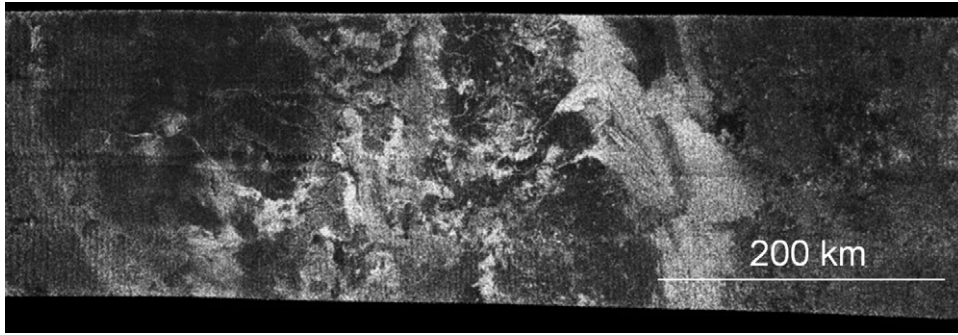
(a)
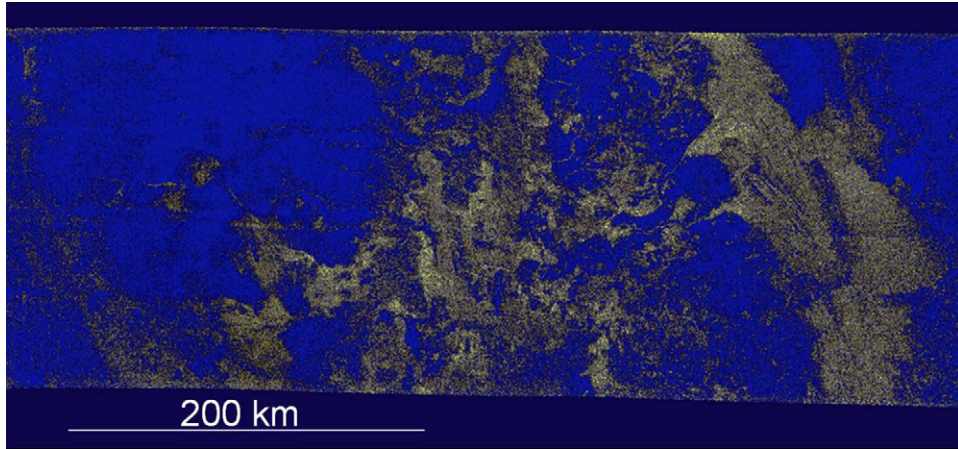
(b)
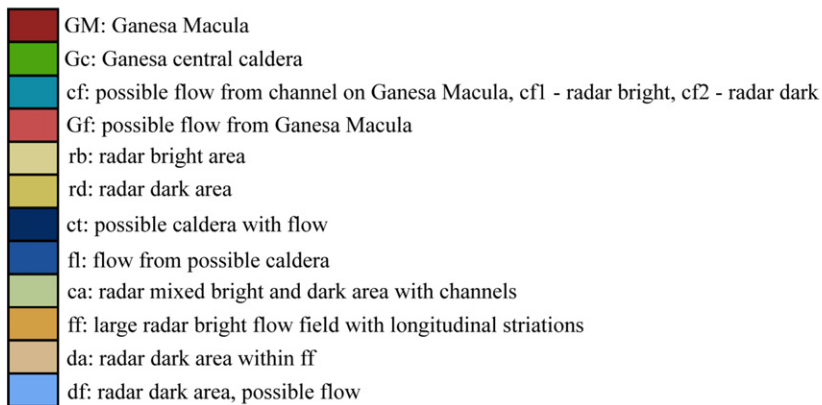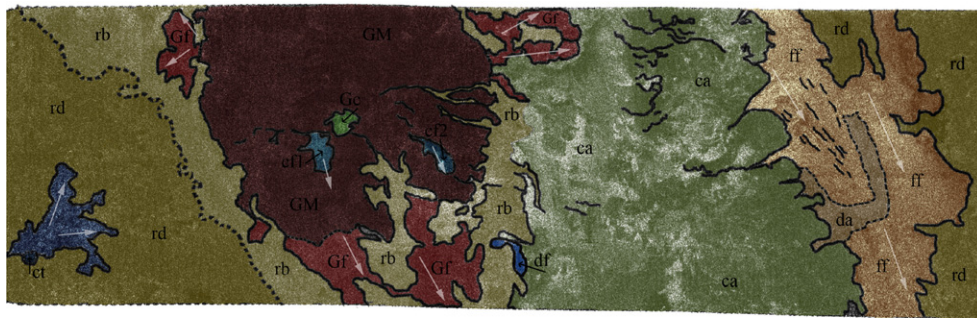
(c)

Fig. 4. (a) Ganesa Macula (left) and region to the east of Ganesa showing many overlapping flow features. Flow directions imply a regional slope to the east. This image was acquired in Ta, the swath is about 200 km high. Ganesa Macula is located at 87° W, 50° N. (b) Gradient map of the Ganesa Macula region with contrast enhancement to show major regional outlines and the complexity of the region east of Ganesa. Radar-dark regions appear in shades of blue, while radar-bright regions appear in shades of yellow (after Reffet et al., 2005). (c) Geologic sketch map of the Ganesa Macula region, showing the main structure (unit GM) and surrounding flows (units cf, Gf, fl, ft). Inferred flow directions are shown by arrows.
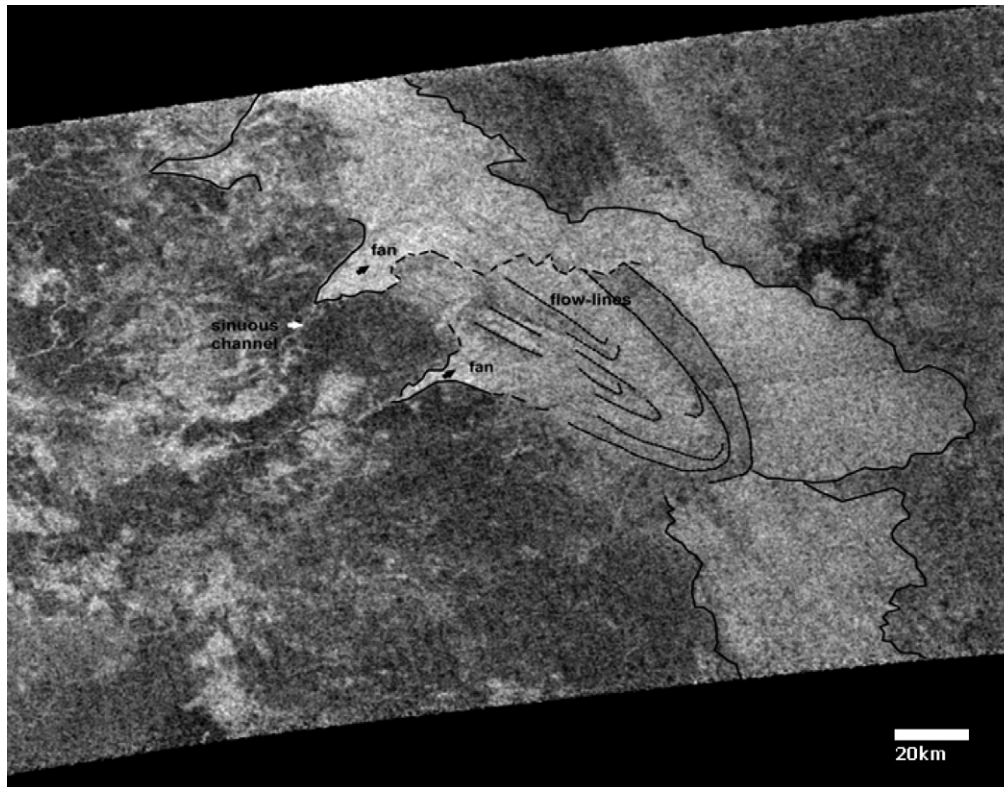
Fig. 5. Flow features east of Ganesa Macula. The SAR-bright fan-like deposits interpreted as either cryovolcanic or alluvial in origin. See Fig. 4 for regional context (from Paganelli et al., 2005).

that pancake-type domes would likely exist on Titan, though no predictions were made for domes as large as Ganesa. Alternatively, Ganesa could be a shield volcano. The morphology and scale of Ganesa are comparable with shield volcanoes on Earth and Venus, and shield volcanoes are common on Earth, Venus, Mars, and the Moon, building as magma erupts from a long lived source. It is possible that Ganesa is a radar-dark shield surrounded by radar-bright (rough) flows at the margins.

If Ganesa Macula is indeed a dome-like construct, it is likely more similar to steep-sided domes on Venus than on Earth. Although steep-sided domes do exist on Earth, they tend to be among the Earth's roughest features (Plaut et al., 2004), due to the fact that the high viscosity lavas form a thick crust that breaks into blocks. In contrast, domes on Venus have steep sides but smooth upper surfaces, suggesting an inability to retain a stable crust that would have broken up into blocks (Stofan et al., 2000).

Studies of the freezing of cryovolcanic domes like Ganesa are underway with a 2-dimensional finite-difference heat conduction code (Neish et al., 2006). In the model, heat is principally lost to the atmosphere through the top of the dome (the atmosphere is held at a constant 95 K), and to the crust through the bottom of the dome. For a dome 1 km in height, it would take 5×10^3 years to freeze for lava made of water, and 12×10^3 years for lava made of ammonia dihydrate (which has a lower freezing temperature). As heat is lost from the dome, the ice layers will grow and the remaining liquid layer will shrink, causing the organics dissolved in it to become more concentrated and

increasing reaction rates. Reaction rates also depend strongly on the temperature (and therefore the ammonia content) of the melt. Significant yields of amino acids could be obtained in a year at 273 K, but reaction rates could be $\sim\!10^6$ times slower at the ammonia–water peritectic temperature of 176 K.

The time available for such chemistry to occur in a cryovolcanic features depends on the size, and, in particular, for wide flat features like Ganesa, on the thickness of the feature. This is not just due to the freezing time (which for a broad, flat feature is proportional to the square of the thickness), but also the temperature-dependent reaction rates in the aqueous liquid. Thus the resultant chemical yields are strongly dependent on the thickness.

3.2. Flow features

We have interpreted extensive deposits with lobate boundaries and relatively uniform radar properties identified in the Titan radar images as flow features, due to their similar radar appearance to flow features on Earth and Venus. Numerous flow features appear to be associated with Ganesa, while several other flow features are seen elsewhere in the Ta swath. Three flows are associated with caldera-like features, while two other flow complexes are associated with either fissure or channel features that may be vents.

3.2.1. Flows east of Ganesa

Numerous flows are located to the east of Ganesa (Figs. 4a–4c). Some flow directions can be mapped (Fig. 4c), but over-

lapping makes it difficult to map individual flows. It is likely that these are flow complexes, made up of multiple flows of similar radar backscatter. A radar-bright flow field is located approximately 180 km from the eastern edge of Ganesa (Fig. 5). The flow field forms three fan-like deposits (unit ft in Fig. 4c), which has led to the suggestion that these may be alluvial in origin (Paganelli et al., 2005), but a cryovolcanic origin is also possible. The fan-like features originate from three narrow channels, indicating a possible change in topography (Fig. 5), possibly a break in slope which allowed the material in the channels to spread out into fans up to approximately 41 km wide. Flow-lines are seen to parallel the flow direction and also to mark lobate flow fronts (Fig. 5). These lines can be drawn within a radar-grayish bounding unit whose arched shape resembles a frontal-moraine-like feature. Outside the bounding radar-grayish unit, the radar-bright materials define flows spreading to the east.

The SAR-bright sinuous channels, associated fan-like features and flows suggest the presence of transported material with different radar properties than the surrounding surfaces. Channels are about 0.5–1 km wide and extend for tens of kilometers, much larger in scale than the channels seen in the Huygens images (Tomasko et al., 2005). The SAR-bright materials forming the fan-like deposits may be associated with a high component of volume backscattering [as suggested by Janssen et al. (2005) and Paganelli, F., Janssen, M.A., West, R., Stiles B., Callahan, P., Lopes, R.M., Stofan, E., Lorenz, R.D., Lunine, J., Kirk, R.L., Roth, L., Wall, S.D., Elachi, C., and the Radar Team, 2006. Titan surface from Cassini RADAR SAR and radiometry data of the first five fly-bys. In preparation], possibly due to a combination of surface roughness and composition in the presence of heterogeneous materials.
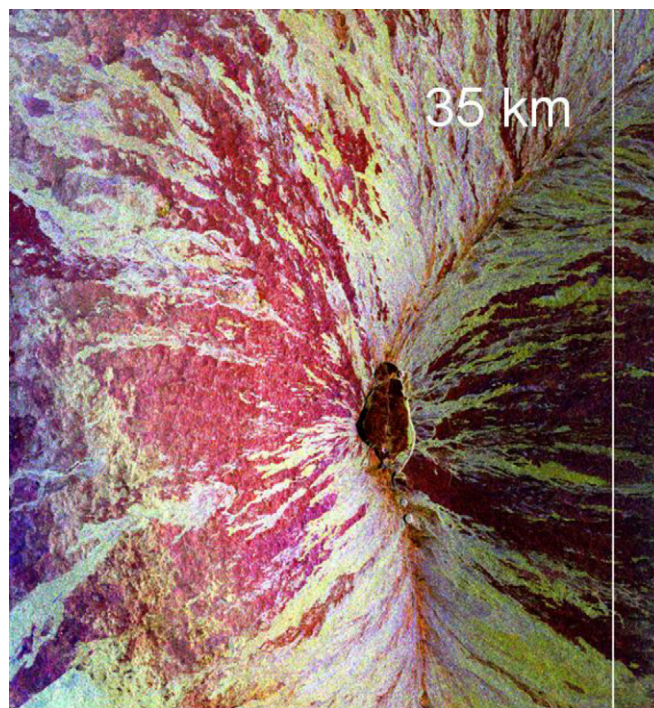
3.2.2. Large flow complex

The largest flow field complex seen in radar images to date is located approximately 1340 km east of Ganesa's eastern edge (Figs. 6a, 6c). The flow extends from 50° W, 52° N to 44° W, 47° N. Several radar-bright flow units can be identified, and this complex appears to be the result of several sources that are either fissures or channels, and are aligned roughly SW–NE to the north of the complex (Fig. 6a); the flows' directions all appear to be to the south and east, in roughly the same direction as the flows nearer Ganesa. This is further evidence of a regional slope in the Ta swath area east of Ganesa, and is the same direction indicated in the first 100 km of the altimetry track obtained east-southeast of the Ta swath (Kirk et al., 2005).

The large flow complex forms a series of lobate deposits, consistent with volcanic flows or sediment laden flows extending beyond the radar coverage both to the north and south. This is an extensive complex, with a minimum area of 23,700 km². Although it is difficult to trace individual flows, we estimate that their lengths are at least 100 km, most likely several hundreds of km. The flow field is similar in size to flow fields on Venus and Mars. For example, the 200 large flow fields identified on Venus range in areal extent from 39,000 to 744,000 km² (Magee and Head, 2001). Of these 200, 41 are not as-
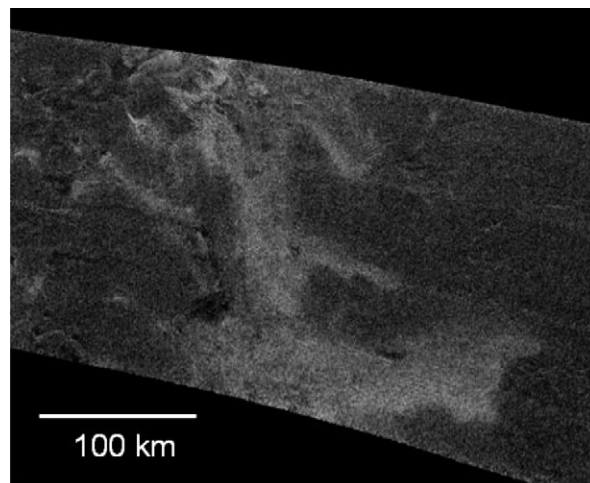
(a)

(b)

Fig. 6. (a) Large flow complex, centered at 45° N, 30° W in the Ta SAR swath. This radar-bright flow complex may have originated from small channels or fissures near the top left of the image, or from a region to the NW not imaged by radar. The flow complex has an area of at least 23,700 km². It likely extends to both to the north (top right) and south (bottom right) of the swath. (b) Mauna Loa imaged from SIR-C. This volcano's many flows are possible morphological analogs to the large flow in Fig. 6, as the flows, fed from a rift zone, are narrow near the vent, and flow long distance, spreading out on the volcano's lower slopes. The different colors in this SIR-C image represent varying roughness. Smoother (pahoehoe) flows are red, rougher (aa) are yellow and white. The rift zone appears orange. The image's height is about 35 km. (Image courtesy of NASA/JPL.) (c) Geological sketch map of area east of Ganesa, showing the large, radar-bright flow (unit fl, also shown in Fig. 6a) and the semi-circular structure (unit pd) that may be a similar construct to Ganesa. The small crater and flow on the right of the map (cf) are shown in Fig. 8. Inferred flow directions are shown by arrows.

sociated with a central shield-type volcano or corona; instead they originate from fractures or are linked spatially to fracture zones or chasmata (Stofan and Smrekar, 2005). It is pos-
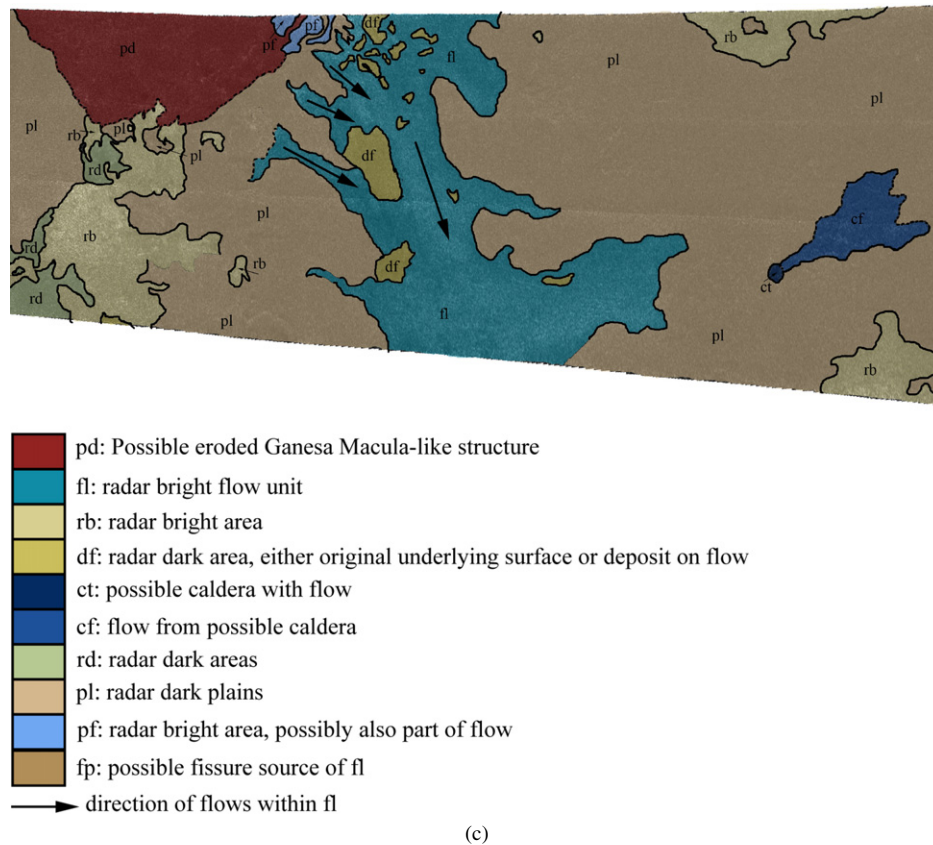
pd: Possible eroded Ganesa Macula-like structure

fl: radar bright flow unit

rb: radar bright area

df: radar dark area, either original underlying surface or deposit on flow

ct: possible caldera with flow

cf: flow from possible caldera

rd: radar dark areas

pl: radar dark plains

pf: radar bright area, possibly also part of flow

fp: possible fissure source of fl

→ direction of flows within fl

(c)

Fig. 6. (*continued*)

sible that this large flow field on Titan originates from a fissure or fracture zone, perhaps similar to the Mauna Loa rift zone on Earth (Fig. 6b). Radar coverage of the area to the north and northwest of the flow field would be needed to identify the type of vent for this flow field. However, mapping of the region (Fig. 6c) shows what is possibly part of a circular structure to the west and northwest of the flow, which may be a similar construct to Ganesa (unit pd in Fig. 6c), though more eroded. This could be the source of the bright flow (unit fl in Fig. 6c), however, images to the north of the current swath are needed to test this tentative interpretation.

We interpret this flow as cryovolcanic in origin, although a fluvial origin cannot be ruled out. Our interpretation is based on the lobate form and morphological similarity to volcanic flows on Earth, the proximity to Ganesa and to a caldera-like feature and flow interpreted as cryovolcanic (units ct and cf in Fig. 6c, see also discussion below), the absence of fluvial networks in the area, and the large size of the flow field. Although no reliable estimate of thickness of this flow could be obtained from radarclinomery (Kirk et al., 2005), if we assume the flow to be at least 1 m in thickness (very low compared to the estimate for the flow from the eastern caldera, see below), the total volume would be $\geqslant 23.7$ km^3. Such volumes are consistent with those predicted by Mitri and Showman (2005). We consider that this large flow field would more likely be emplaced from episodes of cryovolcanism, particularly in an active region, than from rainfall.

3.2.3. Flows associated with calderas

Three circular depressions imaged in Ta have flows emanating from them. Although the possibility that these may be impact craters cannot be eliminated at this time, their irregular shape and emerging flow in one direction (which breaches the rim) supports a volcanic origin, as does the absence of any identifiable ejecta. We refer to these features as calderas because their morphologies are similar to those of calderas on Earth. The feature referred to here as the Eastern caldera (unit ct in Fig. 6c) is close to the large flow complex discussed above, the Western caldera is located near the western end of the Ta swath, in a region of mostly homogeneous terrain, and the Central caldera is to the southwest of Ganesa.
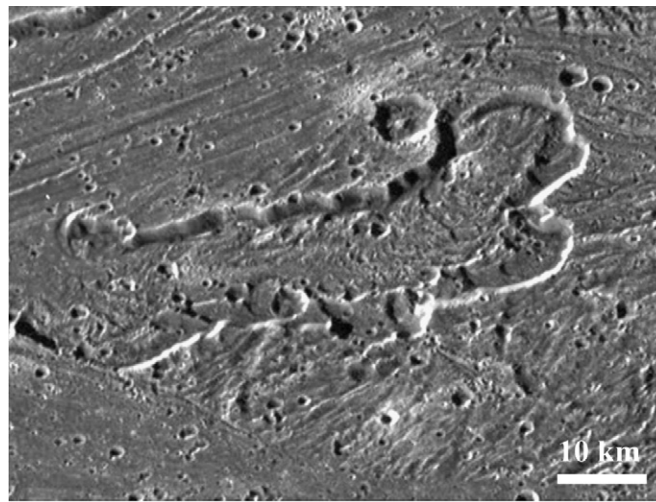
Western caldera and flow   An irregular-shaped crater (Fig. 7a) is seen in the Ta swath about 1070 km from the western edge of Ganesa. The caldera is about 18 km across, with radar-bright rim all around the periphery, indicating rough edges. A flow emanates from the caldera and initially flows to the southwest, then curves and flows to the northwest. It can be traced for about 53 km. Note that this is the only flow feature in the Ta swath that flows west rather than east. This would be consistent with Ganesa being located on a topographic high, but no other data are available at present to evaluate this possibility.

The flow is difficult to map in its entirety, as this part of the radar swath has poor signal/noise and lower spatial resolution than other areas in which flow features are found. The flow is at least 84 km long, and has a minimum area of 1020 km^2
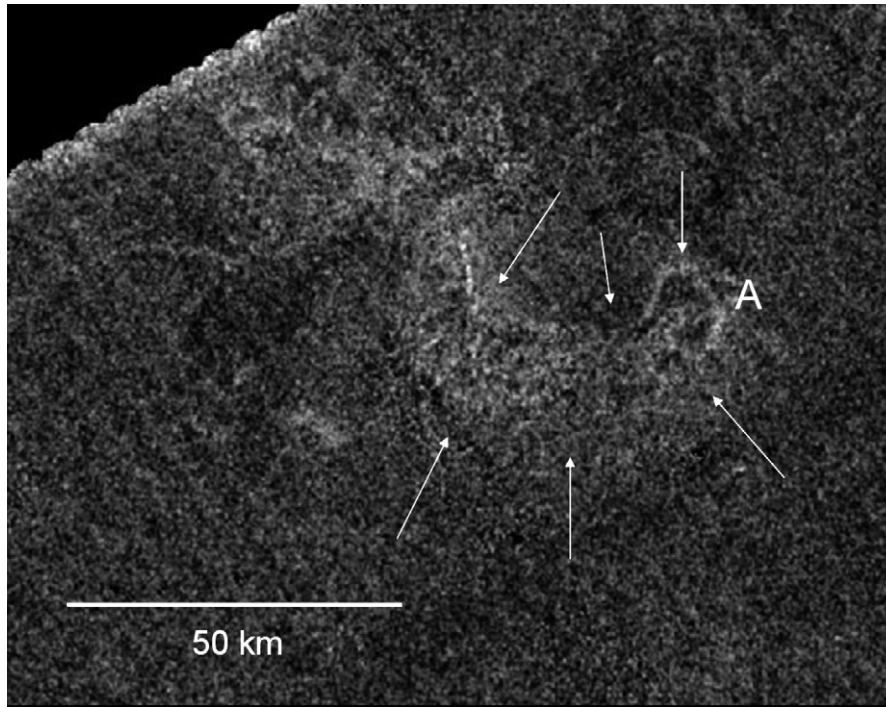
(a)

(b)

Fig. 7. (a) Western caldera and flow. This caldera (labeled A) and associated flow (outlined by arrows) are located near the western end of the Ta SAR swath. The irregularly shaped caldera and change in flow direction are reminiscent of the Prometheus flow field shown in Fig. 9. The radar illumination is from the bottom of the image. The location of the flow's radar bright edge (northern part of the flow) suggests that the flow is in a depression, perhaps similar to the scalloped depression on Ganymede shown in Fig. 10. (b) Caldera-like feature on the grooved terrain on Ganymede, similar in morphology to the Titan feature shown in Fig. 8. The Ganymede scalloped feature has a central deposit and may have flowed to the left (after Prockter, 2004).

and has as a source an irregularly formed source depression, interpreted to be a caldera (roughly oval). However, the radar image shows that the brighter edge of the flow (facing the radar) is on the northern side, suggesting that the flow is in a depression or channel. Also, the flow originates within the caldera, unlike the two other flows (from the Central and Eastern calderas), which appear to initiate at the edges. The quality of the data in this part of the Ta swath is not suited to radarclinometry, so topographic information could not be obtained. This feature is possibly similar to a scalloped depression and flow on Ganymede's grooved terrain (Fig. 7b), inter-

preted as a caldera and associated volcanic flow (Geissler, 2000; Prockter, 2004).

Eastern caldera and flow This bright-rimmed, oval-shaped caldera (Fig. 8) is located at 41° W, 47° N, approximately 1610 km from Ganesa's eastern edge. The caldera is about 13 km in diameter. Like its western counterpart, this caldera also has a radar-bright rim, indicating rough edges. A flow comes out as a thin tongue from the eastern part of the caldera, spreading out down its length. The flow is well-defined and can be easily traced for the first 40 km of its length, after which is seems to
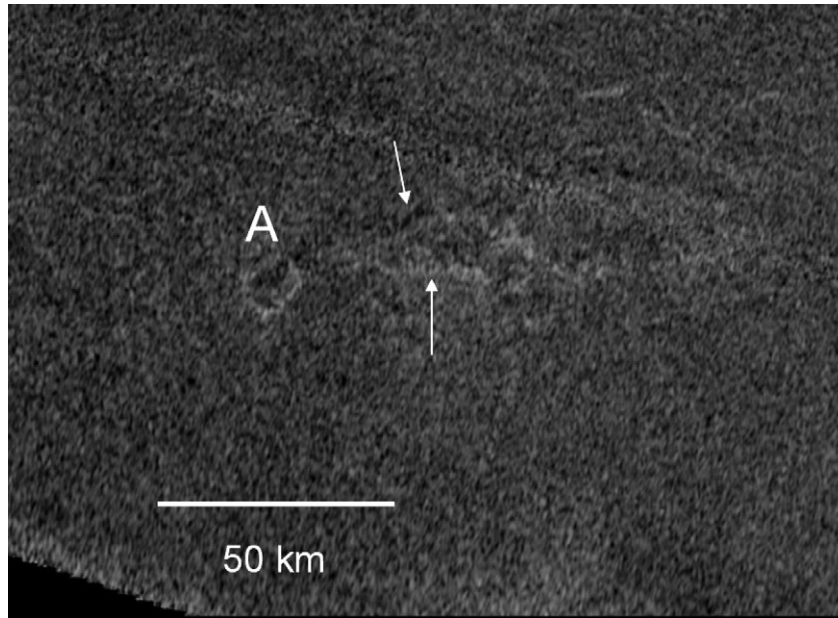
Fig. 8. Eastern caldera and flows. This bright-rimmed caldera (labeled A) and associated flows are located east of Ganesa, at approximately 41° W, 47° N. Note the brighter levees on the side of the flow, indicated by arrows—leveed flows are common on Earth and other planets.

merge into a second, possibly earlier, flow. The area of the combined flows is at least 1230 km². The margins of the younger flow are sufficiently well defined that radarclinometry could be used to estimate the flow thickness in a limited number of places (Kirk et al., 2005), as described further in Section 5.1. Unlike the western flow, this feature has its bright rim on the south, facing the illumination, which suggests that it is elevated rather than occupying a channel.

Central caldera and flow   This is a bright-rimmed and oval caldera (Fig. 9 and unit ct in Fig. 4c), similar to the Eastern caldera, located approximately 115 km west–southwest of the edge of Ganesa. It is about 10 km in diameter, with a narrow flow from the edge heading north–northeast, which fans out approximately halfway along its length (unit fl in Fig. 4c). The flow field outside the crater is mottled, though generally radar-bright, but with no clear bright or dark edges. It appears to fan out into four distinct arms, the first (northern) and third of which are brighter and appear less degraded, and as such are probably younger, than the other two. The combined area of this flow is 1140 km². This flow field is wider relative to its length than either the eastern or western flows, possibly indicating flatter underlying terrain.

3.3. Cryovolcanism and alternative origins

The features described above are all consistent with a cryovolcanic origin. However, this is not a unique interpretation. The features we discussed are of three main types: dome (or shield), calderas with associated flows, and flows associated with channels or with no clear source area imaged.

Ganesa is interpreted as a volcanic construct, a dome or possibly a shield. Topographic data on Ganesa are needed to distinguish between the dome and shield interpretations discussed above. An alternative interpretation that we consider unlikely is that Ganesa is an impact crater. It is a circular feature that is morphologically very different from craters such as the two craters imaged by SAR in T3 (Elachi et al., 2005c). Again, topographic data would provide the definite test of this interpretation.

The second type of proposed cryovolcanic feature, the three caldera-like features that are the sources for flows, are also most likely to be volcanic rather than impact in origin. An impact origin has been ruled out on the basis of the slight noncircularity of the features, and also because, although flows emanating from impact craters are seen distributed around some rampart craters on Mars, the flows here are unidirectional. We also consider a volcanic explosive origin to be unlikely, since Titan's 1.5 bar atmospheric pressure should result in less explosive surficial processes relative to the Earth (and most other planetary bodies), all other factors being equal, resulting in smaller volcanic explosion craters, whereas the observed features are generally larger than the largest explosion craters discovered on the Earth, the Espenberg Maars, at 4–8 km in diameter (Begét et al., 1996).

The third type of feature, the flows in Figs. 5 and 6, are the most challenging to interpret. The flows in Fig. 5 are associated with channels, while those in Fig. 6a have no clear association with a source area, except possibly with a semicircular structure as shown in Fig. 6c. Possibilities for the origin of these flows include cryovolcanism, pluvial/fluvial processes, and mass movement.

Volcanic flows are most easily identified when a source area is visible, such as a crater, caldera, or fissure. Volcanic flows (including cryovolcanic flows of water–ammonia mixtures, which have rheological properties similar to silicate lavas) tend to form lobate deposits, due to relatively high viscosity. However, flows resulting from mass movement and sediment-laden flows
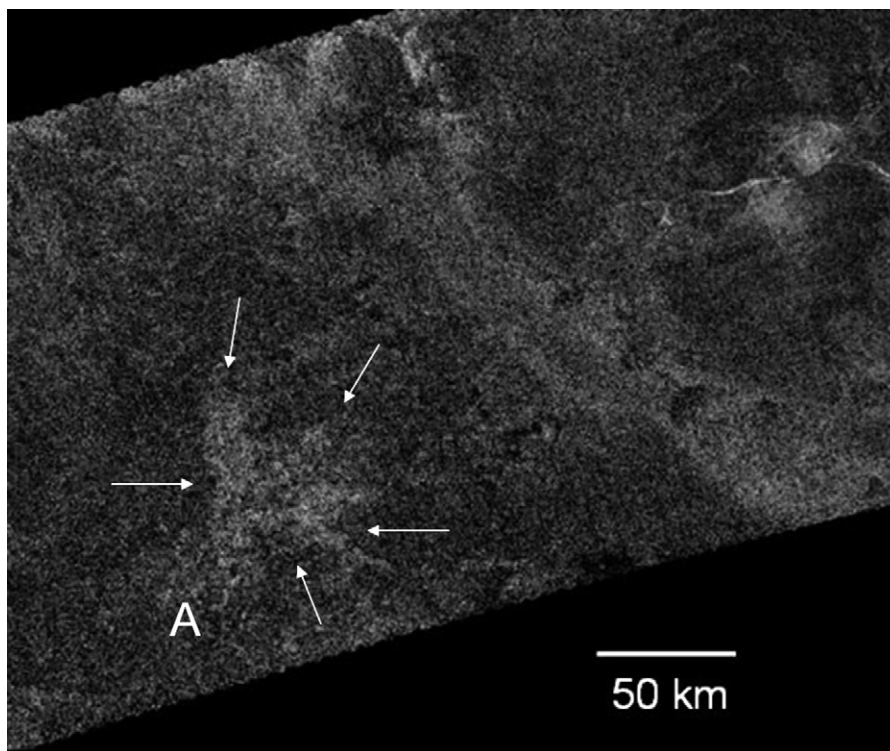
Fig. 9. Central caldera and flows. Part of the Ta swath showing the Central caldera (labeled A) and flow (outlined by arrows) located about 115 km from the western edge of Ganesa. The bright flow appears to be a flow field and is wider than the flows coming out of the western and eastern craters, possibly indicating flatter terrain.

formed from pluvial activity can also form lobate deposits. At the spatial resolution of the radar images, it is difficult to distinguish between these different types of deposits. Detailed topographic data both of the flows and of the terrain are helpful in discriminating between flows formed by different processes, but such data are not yet available for Titan. Cryovolcanic flows, due to the likely rheology of the mixtures involved, would have thick, well-defined margins. Although we cannot at present discriminate between the competing origins for the flows in Figs. 5 and 6a, we consider that mass movement flows are the least likely, as they usually leave behind a characteristic scarp or "crown" region (e.g., Sharpe, 1968) that is not seen associated with the flows discussed here, which appear to be related to channels or fissures. The fan-like deposits in Fig. 6 are associated with channels but are very different in morphology from the alluvial deposits being discussed by Lorenz et al. (2006). Given the lobate morphology of the deposits, their large areas, and their location, near Ganesa and the eastern caldera, we consider that a cryovolcanic origin is the most likely.

## 4. Candidate cryovolcanic features from other fly-bys (T3, T8)

No features that could be positively identified as cryovolcanic in origin were seen on the T3 swath. However, three bright, lobate features might be cryovolcanic in origin. These are shown in Figs. 10a and 10b and they appear to be associated with bright hills and a circular feature (Elachi et al., 2005c). The deposits appear more diffuse than the flows identified in Ta,

which makes our interpretation of their origin more tentative. However, the diffuse appearance could be a result of erosion or partial burial.

The T7 fly-by (at high southern latitudes) did not reveal any features that we interpret as cryovolcanic. The T8 fly-by shows numerous features that could be cryovolcanic. These identifications are, however, tentative at present.

The T8 swath is equatorial and extends from 7° N to 18° S latitude and 179° W to 320° W longitude. Located at the eastern end of the swath are long, parallel ridges that appear to be embayed by the surrounding plains material (Fig. 11). The origin of these ridges is not obvious, but they may be tectonic. Alternatively, they may have been formed by a combination of tectonic and cryovolcanic processes, such as when magma uses a preexisting fracture as an eruption pathway. If the extruded material has a high viscosity, it can form ridge-like features along the fractures.

In the same part of the swath are clusters of small, dark circular features (Fig. 11), which are mostly 1–2 km in diameter. These do not appear to be impact craters, their sizes and morphologies are significantly different from those of the two impact craters so far identified on Titan (Elachi et al., 2005c). Their distribution, though mapped in only a limited area of Titan (Fig. 11), is not characteristic of chains of secondary craters. They show no ejecta blankets and have a modal diameter of 1–2 km, rather than having the broad distribution of sizes that would be expected for impact craters. We suggest that these are collapse or explosion pits, which are common in volcanic regions. The pits could have been formed by heating of methane
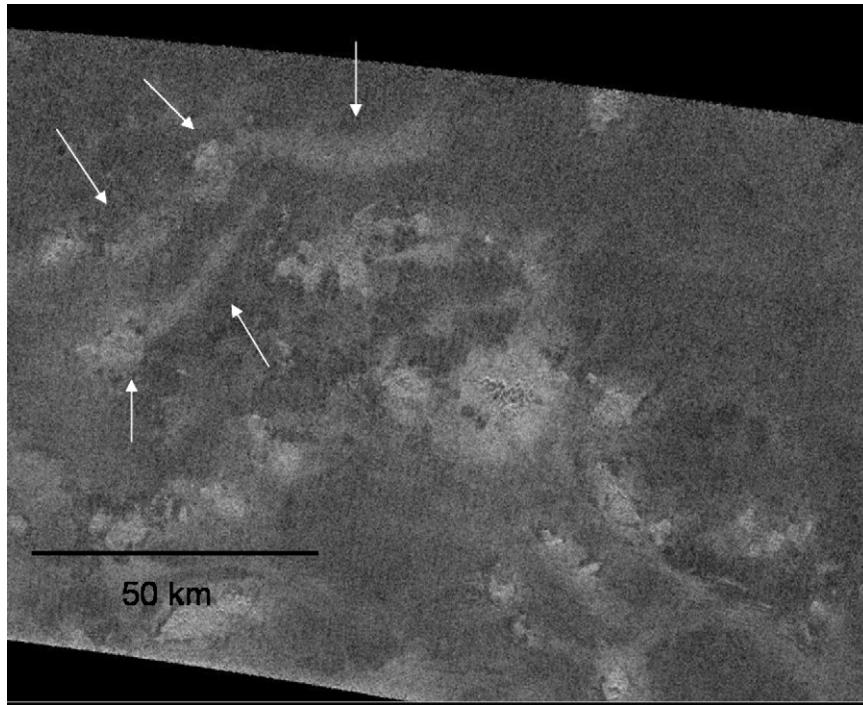
(a)
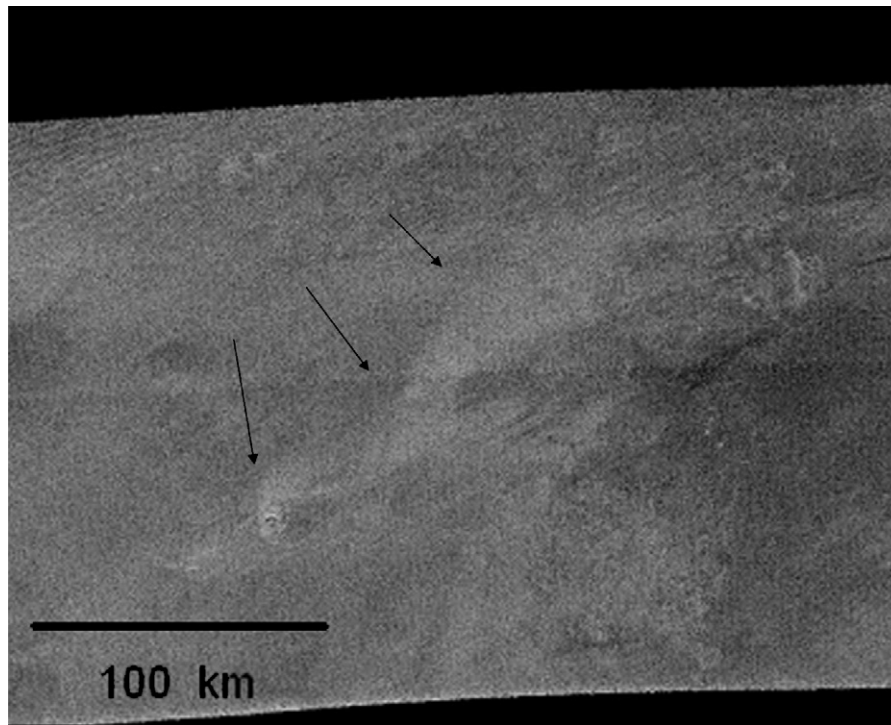
(b)

Fig. 10. (a) Bright, lobate features (indicated by arrows) seen in the T3 SAR swath that may be cryovolcanic in origin. The features appear to be associated with bright, hummocky material that may be small hills. (b) Bright feature seen in the T3 SAR swath interpreted as a possible cryovolcanic flow. The circular feature appears to be a crater and may be the flow source.

pockets by subsurface cryomagmas, perhaps causing explosive ("cryoclastic") activity. Cryoclastic eruptions may have happened on other icy satellites, including Europa (Fagents et al., 2000; see also review by Prockter, 2004), but (as discussed above) it is unclear whether explosive volcanism is likely to be a major process on Titan, and whether its products could be resolved using SAR.

Other features identified in T8 as possibly cryovolcanic in origin are radar-bright, lobate features that appear to be cryovolcanic flows and circular features that may be calderas. One
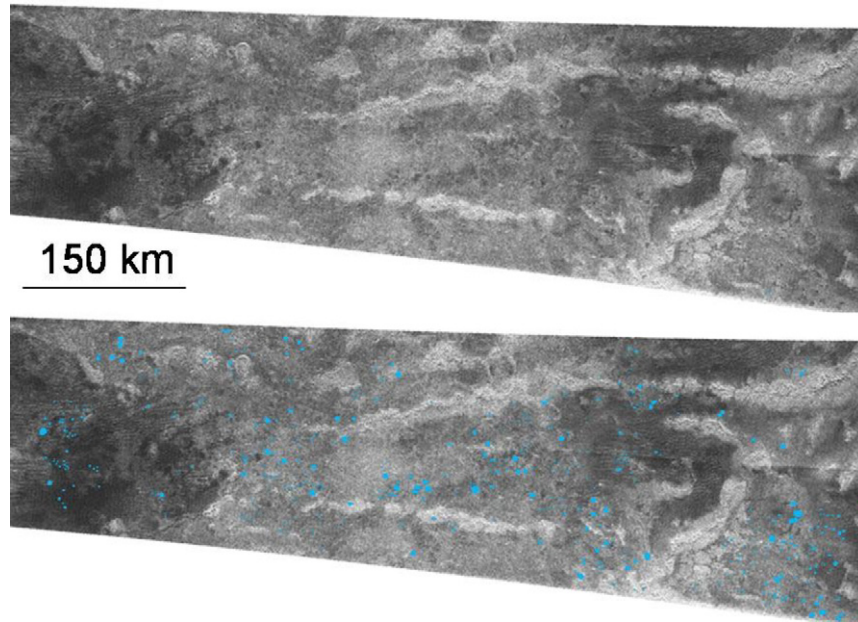
Fig. 11. Possible cryovolcanic features in the T8 swath. Clusters of small, dark circular features mapped (in blue) are mapped in the eastern part of the T8 swath. The SAR image is shown for comparison and is about 200 km high.
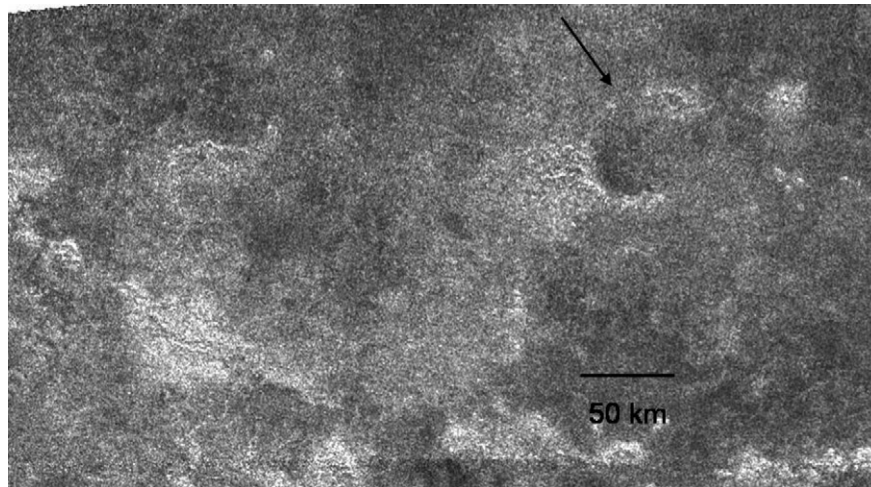

Fig. 12. Possible cryovolcanic feature in the T8 swath. This caldera-like feature (top right) is approximately 60 km in diameter. A bright flow feature is seen to come out of the caldera's southwestern edge.

example of both is shown in Fig. 12, where a radar-bright flow appears to emanate from a circular structure that may be a partially eroded caldera. Some of the bright ridges discussed above are also shown in this image.

5. Possible composition of cryovolcanic materials

The morphology of the candidate cryovolcanic features may provide clues to composition. The final shape of a volcanic flow or construct, such as a dome, is an indication of the rheological properties of materials. According to Kargel (1995), ammonia–water mixtures on Titan (where the gravity is about 1/7 of the Earth's) would produce features similar to those produced by silicate volcanism on Earth and other planets. Ammonia–water

mixtures would be consistent with compositional models for Titan and ammonia would lower the melting point, density, and mobility of liquid water, allowing eruptions to happen more easily. However, the cryolavas on Titan may also include other compounds such as methanol. The composition of cryolavas can have large effect on viscosity. Brines are orders of magnitude less viscous than silicate lavas, while ammonia–water lavas have viscosities similar to silicate lavas

One of the objectives of Cassini is to obtain information about the surface compositions of the satellites. This is especially challenging for Titan because the presence of a substantial atmosphere limits the capability of orbiter instruments to measure surface composition spectroscopically. For example, spectral measurements made by VIMS are constrained within

narrow infrared windows (McCord et al., 2006). In addition, VIMS can only sample the top few microns of the surface, which on Titan may be covered by organics that have been deposited after the formation of the cryovolcanic features and therefore not be representative of the composition of a cryolavas.

Rheological properties, however, can provide additional constraints on composition. In order to derive these properties, measurements of flow dimensions, topography in particular, are needed.

### 5.1. Preliminary rheological analysis of a lava flow

At present, no Radar altimetry is available for the Ta scene. However, the shading of topographic slopes in the SAR image potentially provides additional information about relief at much higher resolution than the Radar operating in altimetric mode, and with a direct connection to specific geologic features, though without the geometric rigor of the altimetry. However, only a small subset of the features seen exhibit the close pairing of bright and dark areas along a profile in range that is characteristic of topographic shading, rather than (or in addition to) the regional brightness differences that result from nontopographic effects such as textural and compositional variations.

Radarclinometry (radar shape-from-shading) can be used to assess the plausibility that such features are truly exhibiting topographic shading, and to estimate their dimensions if so. We have developed a preliminary method of deriving simple, one-dimensional profiles, in which backscatter values on a profile across a feature are interpreted as slopes toward or away from the spacecraft and are integrated to yield an elevation profile (cf. Soderblom et al., 2002, for a similar approach to analysis of visible images). The features of interest are geometrically simple so that clinometry approaches that yield a topographic model over a two-dimensional region (Kirk, 1987; Kirk et al., 2003) are not essential. The analysis requires a model scattering law. A law of the form $\sigma_0 \propto 1/\sin(i)$ closely fits the backscatter of uniform plains in the SAR image over a range of incidence angles $5° < i < 45°$. For our radarclinometric analysis, this function was modified to have the form $\sigma_0 \propto 1/\tan(i)$. The behavior of the two functions at small incidence angles is similar, but the latter is more plausible physically at large incidence angles, in that the backscatter becomes zero as the incidence angle reaches $90°$. The constant of proportionality is chosen independently to give an overall level surface (unless another assumption can be utilized) for each feature modeled.

Our modeling has primarily addressed the eastern caldera flow in the Ta swath, described above, for which the evidence for slope-related shading is clearest. This flow consists of two sequential lobes, each ∼40 km in length, emanating from a bright-rimmed circular feature (41° W, 47° N) interpreted as a caldera (Fig. 13a). It exhibits an unusually bright near-edge and dark far-edge across the flow, and appears to be relatively photometrically uniform, so is a prime candidate for morphometric analysis using a prototype radarclinometric method. A radarcli-
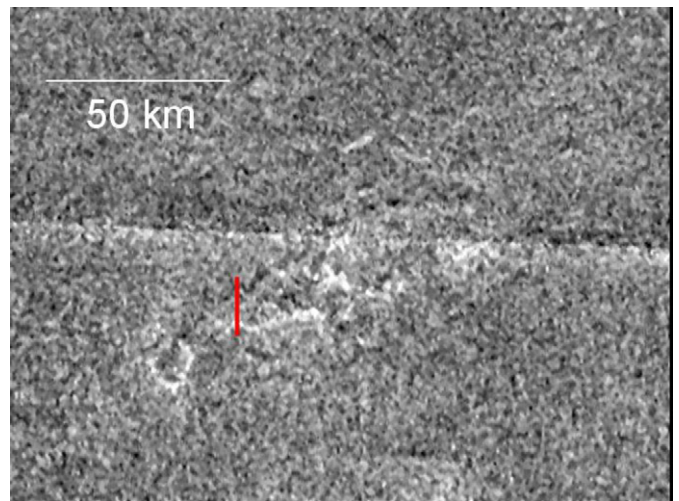
(a)
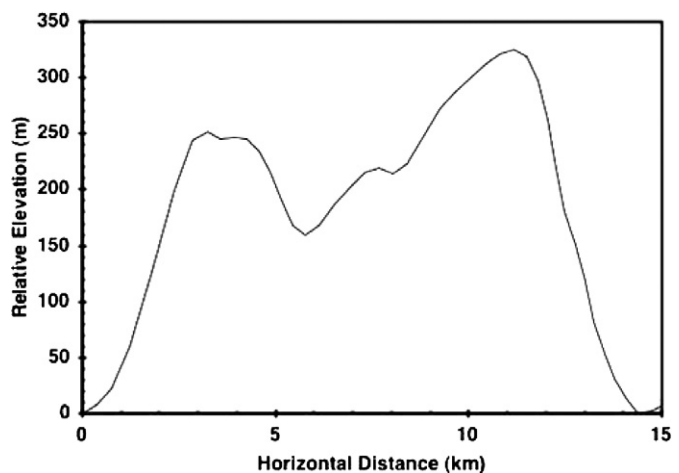
(b)
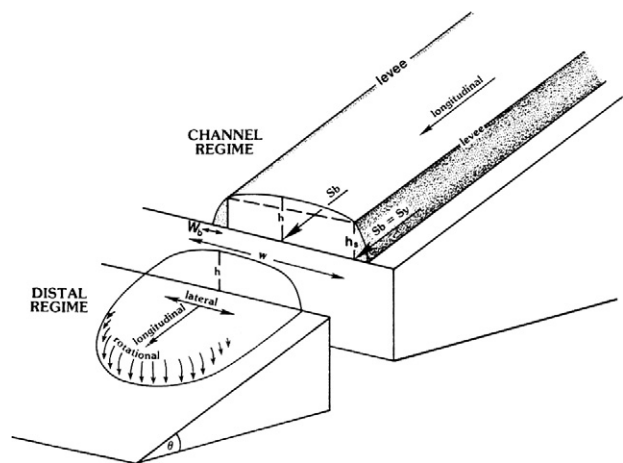
(c)

Fig. 13. (a) Eastern caldera and flow, showing location of photoclinometry profile in red. (b) Radarclinometry profile across the flow shown in (a). Adapted from Kirk et al. (2005). (c) Schematic representation of a lava flow following the model of Hulme (1974). Adapted from Wadge and Lopes (1991).

nometric profile (Fig. 13b) across the flow indicates that it is 200–300 m high with maximum slopes on the order of 7° on both edges. As reconstructed, the top surface of the flow is rela-

tively flat but tilted ∼2°. A more likely interpretation is that the top surface of the flow simply has slightly enhanced backscatter at a given incidence angle compared to the sides.

Cross-flow slopes are only of limited use in analyzing the properties of a lava flow. However, assuming Bingham-like behavior (e.g., Hulme, 1974; Pinkerton and Wilson, 1994; see also Fig. 13c) and that the slopes derived are reliable, the yield strength, S_y, of lava flows can be related to the flow dimensions by the following equations (Hulme, 1974):

$$S_y = \rho g h^2 / w, \tag{1}$$

where ρ is the bulk density, assumed to be 1000 kg m^{-3}, g is the gravity ($\sim$1.35 m s^{-2}), h is the flow height, and w is the flow width (Fig. 13c). The apparent central channel implies that deflation has taken place, and so we must estimate the height when the flow was active, which is assumed to be equal to the top of the levees. There is considerable uncertainty in the data, but using the above relationship we derive an effective yield strength of $\sim$10^4 Pa. If we assume that the flow structure is controlled by bulk rheology then, given a high degree of correlation between yield strength and viscosity as observed for silicate lavas (Pinkerton and Wilson, 1994; Ellis et al., 2004), we can infer viscosities in excess of 10^4 Pa s, albeit with considerable uncertainty; cf. the experimental work of Kargel (e.g., Kargel et al., 1991), who found viscosities of up to $\sim$10^1 Pa s for ammonia–water mixtures and $\sim$10^4 Pa s for ammonia–water–methanol mixtures, as well as terrestrial basalts (200–2.3 × 10^5 Pa s) and andesites (10^5–10^9 Pa s). From this perspective, therefore, the flow exhibits rheological properties inconsistent with ammonia–water slurries, and perhaps more consistent with ammonia–water–methanol slurries.

Caution must be used as some of the assumptions have not been tested. In particular, the assumption that bulk rheology controls the final flow structure is based on a terrestrial silicate volcanism analogue. This model is applicable to some but not all lava flows on Earth (Wadge and Lopes, 1991).

Cooling of the flow may be dramatically accelerated if it occurred within a liquid-hydrocarbon-filled basin that is no longer present, leading to the Titan analog of pillow lavas (Lorenz, 1996). Indeed, evidence from the Huygens landing site for liquid methane and ethane just beneath the visible surface (Niemann et al., 2005) suggests that quenching of the outer boundary of the lava by liquid hydrocarbons might occur even in the absence of a large-scale body of liquid. The procedure described above would then overestimate the effective viscosity of the flow, but is still useful in providing an upper bound. It will be interesting to see if flows seen in future radar images yield lower viscosities, which could imply a heterogeneous distribution of hydrocarbon liquids in contact with ammonia–water or ammonia–water–methanol flows.

6. Energetic limits on extent and timing of cryovolcanism

The total heat flow available today within Titan is 6 mW/m^2, including accretional, radiogenic and tidal heating associated with the noncircularity of Titan's orbit (Sohl et al., 1995). Most of the deep heat flux maintains the interior at an elevated temperature and we assume is not available to melt near-surface ices and generate volcanism. We turn instead to tidal heating, limited to 10% of the total heat flow by the requirement to avoid circularizing Titan's orbit over geologic time (Tobie et al., 2005). While plumes of warm ice may rise buoyantly in a convective icy crust, in the absence of tidal heating they will be stopped by an overlying conductive lid and at best cause doming; tidal dissipation in the plume core instead may allow a melt lens to form at the head of the plume (Sotin et al., 2002).

The argument we present here follows that of Lorenz (1996), though with some updated numbers. We assume that the liquid lens is neutrally buoyant, which requires an ammonia–water melt rather than a pure water system (Croft et al., 1988), and that the melt can rise through cracks to be expressed as surface volcanism or near-surface magmatism. The tidal heating must raise the temperature from the ambient value at the conductive-convective interface and melt the fluid; the maximum rate of volcanic resurfacing per unit area is then

$$R = F_{\text{tidal}} / (L + C \Delta T), \tag{2}$$

where F_{tidal} is the tidal heat flux, L the latent heat of melting of the water, C the specific heat and ΔT the temperature rise. For $F_{\text{tidal}} = 10\%$ of the total heat flux (consistent with the model of Grasset et al., 2000), L equal to the melting of pure water ice (an upper limit), $\Delta T = 100$ K (probably an overestimate), and an assumed 10% conversion efficiency of crustal heat to volcanism as for the Earth (Francis, 1993) we find $R \sim 10^{-10}$ kg/m^2/s. This translates into an upper limit for the layer depth, over the age of the Solar System, of 10 km. However, recent models of the thermal evolution of Titan suggest that a convectively unstable Ice-I layer has been present near surface for only the last 0.5–1 billion years (Tobie et al., 2006), which would imply an upper limit of order 1 km. The production rate of stratospheric photochemical debris is $\sim$10^{-12} kg/m^2/s, two orders of magnitude lower.

We conclude, therefore, that from an energetic point of view it is possible for volcanic resurfacing to dominate over photochemical burial of the surface and, during the last billion years, crustal features could have been reworked or erased on a global scale by ammonia–water flows. The extent to which the surface has actually been reworked by cryovolcanism will need to be assessed with additional observations from the Cassini Titan Radar Mapper and other remote sensing systems. Our calculated volcanic resurfacing rate is an upper limit; lower values will be obtained by virtue of a lesser amount of ammonia available to provide buoyant, viscous volcanic fluids, lower levels of tidal heating, and inefficiencies associated with freezing in cracks during propagation of fluids to the surface. Further, methane and its photochemical products are intrinsically mobile as liquids circulating through the solid crust or evaporating and condensing in meteorological cycles, and as particulates blown by the winds and transported by liquids. We therefore should expect to see large areas buried by organic solids or reworked by light hydrocarbon liquids even in the presence of a prodigious cryovolcanic eruption rate. The view of Titan provided by radar—large areas covered by radar-dark material in-

terrupted by brighter features consistent with water ice—bears out this expectation of complexity created by these competing processes (Elachi et al., 2005b, 2005c).

7. Discussion

If the Ta SAR swath is showing a typical landscape on Titan, we can expect that many other cryovolcanic features will be found elsewhere on Titan during future fly-bys. Present-day cryovolcanic activity is feasible, though it has not been observed. Detection of active cryovolcanism, if any exists, can be attempted by searching for surface changes in overlapping SAR swaths from different fly-bys, however, during the nominal mission, we expect the overlap between SAR swaths to be very limited ($<1\%$ of the surface). Surface changes can potentially also be detected using comparisons between SAR images and data from other remote sensing instruments on Cassini, particularly from VIMS.

The high concentration of volcanic landforms in the Ta strip, in contrast to T3 and T7, leads to the question whether the area around Ganesa might have an unusually high concentration of volcanic features, but much greater surface coverage is needed to examine this possibility. On Mars, the majority of volcanism has occurred on two volcanic provinces: Tharsis and Elysium. The apparent trend of flows away from Ganesa throughout the whole scene is indicative of a broad scale bulge, making the comparison attractive. Given the suggestion that Ganesa may be similar to pancake domes on Venus, perhaps a more appropriate analogue would be that of a large topographically positive corona, which can be as broad as 1100 km across, and typically contain numerous smaller volcanic features, including steep-sided domes.

The findings from the first SAR swath indicate that effusive cryovolcanic features may be common on the surface. Cryovolcanism may be an important resurfacing mechanism on Titan, as discussed above. Based on the small number of impact craters detected to date, the ~6% of Titan's surface imaged by radar to date is very young compared with those from other saturnian satellites. Other instruments on Cassini, notably ISS and VIMS, have not detected additional impact craters so far, though their coverage of the surface is much larger than we have obtained with the radar instrument. We can conclude from these data that widespread resurfacing has occurred and cryovolcanism has likely been an important contributing process.

The topography of cryovolcanic features, though limited at present because of the available data, is of great importance for understanding the rheology and, by inference, the chemical composition, of cryomagmas on Titan. Therefore, accurate topographical measurements of cryovolcanic regions are important for future studies and will be a focus of future investigations.

Cryovolcanic topography is also potentially significant for astrobiology, because the time available for protobiologic chemical reactions (e.g., the conversion of nitriles to amino acids) to occur in cryovolcanic constructs is strongly dependent on their thicknesses (as discussed in Section 3.1). Furthermore, organic compounds formed in Titan's atmosphere will eventually condense and settle to the surface. If these compounds are exposed to liquid water, through cryovolcanism or impact melt, aqueous chemistry can proceed (Thompson and Sagan, 1992; Lorenz et al., 2001; also see Section 3.1). The nitriles and hydrocarbons can then form more evolved and oxidized prebiotic species such as urea, amino acids and nucleotide bases. A goal for future missions to Titan would therefore be to determine insitu the composition of features identified to be cryolavas from morphology. As well as of volcanological/rheological interest, such sites are of chemical interest due to the astrobiological implications.

References

Begét, J.E., Hopkins, D.M., Charron, S.D., 1996. The largest known maars on Earth, Seward Peninsula, northwest Alaska. Arctic 49 (1), 62–69.

Croft, S.K., Lunine, J.I., Kargel, J., 1988. Equations of state of the ammonia–water liquid: Derivation and planetological applications. Icarus 73, 279–293.

Crumpler, L.S., Aubele, J.C., Senske, D.A., Keddie, S.T., Magee, K.P., Head, J.W., 1997. Volcanoes and centers of volcanism on Venus. In: Brougher, S.W., Hunten, D.M., Phillips, R.J. (Eds.), Venus II. Univ. of Arizona Press, Tucson, AZ, pp. 697–756.

Elachi, C., Allison, M.D., Borgarelli, L., Encrenaz, P., Im, E., Janssen, M.A., Johnson, W.T.K., Kirk, R.L., Lorenz, R.D., Lunine, J.I., Muhleman, D.O., Ostro, S.J., Picardi, G., Posa, F., Rapley, C.G., Roth, L.E., Seu, R., Soderblom, L.A., Vetrella, S., Wall, S.D., Wood, C.A., Zebker, H.A., 2005a. RADAR: The Cassini Titan Radar Mapper. Space Sci. Rev. 117, 71–110.

Elachi, C., Wall, S., Allison, M., Anderson, Y., Boehmer, R., Callahan, P., Encrenaz, P., Flamini, E., Francescetti, G., Gim, Y., Hamilton, G., Hensley, S., Janssen, M., Johnson, W., Kelleher, K., Kirk, R., Lopes, R., Lorenz, R., Lunine, J., Muhleman, D., Ostro, S., Paganelli, F., Picardi, G., Posa, F., Roth, L., Seu, R., Shaffer, S., Soderblom, L., Stiles, B., Stofan, E., Vetrella, S., West, R., Wood, C., Wye, L., Zebker, H., 2005b. First views of the surface of Titan from the Cassini RADAR. Science 308, 970–974.

Elachi, C., Wall, S., Janssen, M., Stofan, E., Lopes, R., Kirk, R., Lorenz, R., Lunine, J., Paganelli, F., Soderblom, L., Wood, C., Wye, L., Zebker, H., Anderson, Y., Ostro, S., Allison, M., Boehmer, R., Callahan, P., Encrenaz, P., Flameni, E., Francescetti, G., Gim, Y., Hamilton, G., Hensley, S., Johnson, W., Kelleher, K., Muhleman, D., Picardi, G., Posa, F., Roth, L., Seu, R., Schaffer, S., Stiles, B., Vetrella, S., West, R., 2005c. Titan Radar Mapper observations from Cassini's Ta and T3 fly-bys. Nature 441 (8), 709–713, doi:10.1038/nature0486.

Ellis, B., Wilson, L., Pinkerton, H., 2004. Estimating the rheology of basaltic lava flows. Lunar Planet. Sci. 35. Abstract 1550.

Fagents, S.A., Greeley, R., Sullivan, R.J., Pappalardo, R.T., Prockter, L.M., the Galileo SSI Team, 2000. Cryomagmatic mechanisms for the formation of

Rhadamanthys Linea, triple band margins, and other low-albedo features on Europa. Icarus 144, 54–88.

Fink, J.H., Bridges, N.T., Grimm, R.E., 1993. Shapes of venusian "pancake" domes imply episodic emplacement and silicic composition. Geophys. Res. Lett. 20 (4), 261–264.

Francis, P., 1993. Volcanoes: A Planetary Perspective. Oxford Univ. Press, Oxford, UK.

Fortes, A.D., Grinrod, P.M., 2006a. A sulfate-rich model of Titan's interior. 1. Implications for the composition of cryomagmas. Lunar Planet. Sci. 37. Abstract 1293.

Fortes, A.D., Grindrod, P.M., 2006b. Modeling of possible mud volcanism on Titan. Icarus 182, 550–558.

Geissler, P., 2000. Cryovolcanism in the Solar System. In: Sigurdsson, H., et al. (Eds.), Encyclopedia of Volcanoes. Academic Press, San Diego, pp. 785–800.

Grasset, O., Sotin, C., 1996. The cooling rate of a liquid shell in Titan's interior. Icarus 123, 101–112.

Grasset, O., Sotin, C., Deschamps, F., 2000. On the internal structure and dynamics of Titan. Planet. Space Sci. 48, 617–636.

Grindrod, P.M., Fortes, A.D., 2006. A sulfate-rich model of Titan's interior. 2. Implications for explosive volcanism. Lunar Planet. Sci. 37. Abstract 1294.

Hulme, G., 1974. The interpretation of lava flow morphology. Geophys. J. R. Astron. Soc. 39, 361–383.

Janssen, M.A., Paganelli, F., Kirk, R., Lorenz, R.D., Lopes, R.M., the Cassini RADAR Team, 2005. Titan's surface properties from the Cassini RADAR radiometer. Bull. Am. Astron. Soc. 37, 739.

Kargel, J.S., 1995. Cryovolcanism on the Icy satellites. Earth Moon Planets 67, 101–113.

Kargel, J.S., Croft, S., Lunine, J., Lewis, J., 1991. Rheological properties of ammonia–water liquids and crystal slurries: Planetological implications. Icarus 89, 93–112.

Kirk, R.L., 1987. A fast finite-element algorithm for two-dimensional photoclinometry. Ph.D. thesis, Caltech.

Kirk, R.L., Barrett, J.M., Soderblom, L.A., 2003. Photoclinometry made simple. In: Advances in Planetary Mapping 2003, Houston, Texas. Available online at http://astrogeology.usgs.gov/Projects/ISPRS/MEETINGS/Houston2003/abstracts/Kirk_isprs_mar03.pdf.

Kirk, R.L., Callahan, P., Seu, R., Lorenz, R.D., Paganelli, F., Lopes, R., Elachi, C., Cassini RADAR Science Team, 2005. RADAR reveals Titan's topography. Lunar Planet. Sci. 36. Abstract 2227.

Lopes, R.M.C., Kilburn, C.R.J., 1990. Emplacement of lava flows fields: Application of terrestrial studies to Alba Patera, Mars. J. Geophys. Res. 95 (B9), 14383–14397.

Lorenz, R.D., 1993. The surface of Titan in the context of ESA's Huygens probe. ESA J. 17, 275–292.

Lorenz, R.D., 1996. Pillow lava on Titan: Expectations and constraints on cryovolcanic processes. Planet. Space Sci. 44 (9), 1021–1028.

Lorenz, R., Mitton, J., 2002. Lifting Titan's Veil. Cambridge Univ. Press, Cambridge, UK. 260 pp.

Lorenz, R.D., Lunine, J.I., McKay, C.P., 2001. Geological settings for aqueous synthesis on Titan revisited. Enantiomer 6, 83–96.

Lorenz, R.D., Lopes, R.M., Paganelli, F., Lunine, J.I., Kirk, R.L., Soderblom, L.A., Stofan, E.R., Ori, G., Myers, M., Miyamoto, H., Stiles, B., Wall, S.D., Wood, C.A., Cassini RADAR Team, 2006. Fluvial channels on Titan: Meteorological paradigm and Cassini RADAR observations. Planet. Space Sci. Submitted for publication.

Magee, K.P., Head III, J.W., 2001. Large flow fields on Venus: Implications for plumes, rift associations, and resurfacing. In: Ernst, R.E., Buchan, K.L. (Eds.), Mantle Plumes: Their Indentification Through Time. Special Paper 352. Geol. Soc. Am., Boulder, CO, pp. 81–101.

McCord, T., Hansen, G.B., Buratti, B.J., Clark, R.N., Cruikshank, D.P., D'Aversa, E., Griffith, C.A., Baines, K.H., Brown, R.H., Dalle Ore, C.M., Filacchione, R.M., Formisano, V., Hibbits, C.A., Jaumann, R., Lunine, J.I., Nelson, R.M., Sotin, C., Cassini VIMS Team, 2006. Composition of Titan's surface from Cassini VIMS. Planet. Space Sci. Submitted for publication.

McKenzie, D., Ford, P.G., Liu, F., Pettengill, G.H., 1992. Pancake-type domes on Venus. J. Geophys. Res. 97 (E8), 15967–15976.

McKinnon, W.B., 2006. On convection in ice I shells of outer Solar System bodies, with detailed application to Callisto. Icarus 183, 435–450.

Mitri, G., Showman, A.P., 2005. Convective–conductive transitions and sensitivity of a convecting ice shell to perturbations in heat flux and tidal-heating rate: Implications for Europa. Icarus 177, 447–460.

Mitri, G., Lunine, J.I., Showman, A.P., Lopes, R., 2006. Resurfacing of Titan by ammonia–water cryomagma. Icarus. Submitted for publication.

Neish, C.D., Lorenz, R.D., O'Brien, D.P., Cassini RADAR Team, 2006. The potential for prebiotic chemistry in the possible cryovolcanic dome Ganesa Macula on Titan. Int. J. Astrobiol. 5 (01), 57–65.

Niemann, H.B., Atreya, S.K., Bauer, S.J., Carignan, G.R., Demick, J.E., Frost, R.L., Gautier, D., Haberman, J.A., Harpold, D.N., Hunten, D.M., Israel, G., Lunine, J.I., Kasprzak, W.T., Owen, T.C., Paulkovich, M., Raulin, F., Raaen, E., Way, S.H., 2005. Huygens Probe gas chromatograph mass spectrometer: The atmosphere and surface of Titan. Nature 438, 779–784, doi:10.1038/nature04122.

Paganelli, F., Elachi, C., Lopes, R.M., Stofan, E., Wood, C.A., Janssen, M.A., Stiles, B., West, R., Roth, L., Wall, S.D., Lorenz, R.D., Lunine, J.I., Kirk, R.L., Soderblom, L., Cassini Radar Team, 2005. Channels and fan-like features on Titan's surface imaged by the Cassini RADAR. Lunar Planet. Sci. 36. Abstract 2150.

Pavri, B., Head III, J.W., Klose, K.B., Wilson, L., 1992. Steep-side domes on Venus: Characteristics, geological setting, and eruption conditions from Magellan data. J. Geophys. Res. 97, 13445–13478.

Pinkerton, H., Wilson, L., 1994. Factors controlling the lengths of channel-fed lava flows. Bull. Volcanol. 56 (2), 108–120.

Prockter, L., 2004. Ice volcanism on Jupiter's moons and beyond. In: Lopes, R.M.C., Gregg, T.K.P. (Eds.), Volcanic Worlds: Exploring the Solar System Volcanoes. Praxis Publishing, Chichester, pp. 145–177.

Plaut, J.J., Anderson, S.W., Crown, D.A., Stofan, E.R., van Zyl, J.J., 2004. The unique radar properties of silicic lava domes. J. Geophys. Res. 109, doi:10.1029/2002JE002917. E03001.

Reffet, E.G., Boubin, G.M., Lunine, J., Radebaugh, J., Lopes, R.M., 2005. Cassini Radar Team cryovolcanic features on Titan: Interpretation of Cassini Radar Data. In: 37th American Astronomical Society Division for Planetary Sciences Meeting, 4–6 September 2005, Cambridge, UK.

Roe, H.G., Brown, M.E., Schaller, E.L., Bouchez, A.H., Trujillo, C.A., 2005. Geographic control of Titan's mid-latitude clouds. Science 310, 477–479.

Roberts, K.M., Guest, J.E., Head, J.W., Lancaster, M.G., 1992. Mylitta Fluctus, Venus: Rift-related, centralized volcanism and the emplacement of large-volume flow units. J. Geophys. Res. 97, 15991–16016.

Sharpe, C.F.S., 1968. Landslides and Associated Phenomena. Cooper Square, New York.

Soderblom, L.A., Kirk, R.L., Herkenhoff, K.E., 2002. Accurate fine-scale topography for the martian south polar region from combining MOLA profiles and MOC NA images. Lunar Planet. Sci. 33. Abstract 1254.

Sohl, F., Sears, W., Lorenz, R.D., 1995. Tidal dissipation on Titan. J. Geophys. Res. 115, 278–294.

Sotin, C., Head III, J.W., Tobie, G., 2002. Tidal heating of upwelling thermal plumes and the origin of lenticulae and chaos melting. Geophys. Res. Lett. 29 (8), doi:10.1029/2001GL013844. 1233.

Sotin, C., Jaunmann, R., Buratti, B.J., Brown, R.H., Clark, R.N., Soderblom, L.A., Baines, K.H., Bellucci, G., Bribing, J.-P., Capaccioni, F., Cerroni, P., Coradini, A., Cruikshank, D.P., Drossart, P., Formisano, V., Langevin, Y., Matson, D.L., McCord, T.B., Nelson, R.M., Nicholson, P.D., Sicardy, B., LeMouelic, S., Rodriguez, S., Stephan, K., Scholz, C.K., 2005. Release of volatiles from a possible cryovolcano from near-infrared imaging of Titan. Nature 435, 786–789.

Stevenson, D.J., 1992. Interior of Titan. In: Proceedings of the Symposium on Titan, Toulouse, France, 12 September 1991. European Space Agency, Noordwijk, the Netherlands, p. 2933.

Stofan, E.R., Anderson, S.W., Crown, D.A., Plaut, J.J., 2000. Emplacement and composition of steep-sided domes on Venus. J. Geophys. Res. 105, 26757–26772.

Stofan, E.R., Smrekar, S.E., 2005. Large topographic rises, coronae, large flow fields and large volcanoes on Venus: Evidence for mantle plumes? Special Paper Geol. Soc. Am., Boulder, CO, 388. pp. 841–861.

Thompson, R.W., Sagan, C., 1992. Organic chemistry on Titan—Surface interactions. In: Proceedings of the Symposium on Titan, Toulouse, September

1991. ESA SP-338. European Space Agency, Noordwijk, the Netherlands, pp. 167–182.

Tobie, G., Grasset, O., Lunine, J.I., Mocquet, A., Sotin, C., 2005. Titan's internal structure inferred from a coupled thermal–orbital model. Icarus 175, 496–502.

Tobie, G., Lunine, J.I., Sotin, C., 2006. Episodic outgassing as the origin of atmospheric methane on Titan. Nature 440 (2), 61–64, doi:10.1038/nature04497.

Tomasko, M.G., Archinal, B., Becker, T., Bézard, B., Bushroe, M., Combes, M., Cook, D., Coustenis, A., de Bergh, C., Dafoe, L.E., Doose, L., Douté, S., Eibl, A., Engel, S., Gliem, F., Grieger, B., Holso, K., Howington-Kraus, A., Karkoschka, E., Keller, H.U., Kirk, R., Kramm, R., Küppers, M., Lellouch, E., Lemmon, M., Lunine, J., McFarlane, E., Moores, J., Prout, M., Rizk, B., Rosiek, M., Rüffer, P., Schröder, S.E., Schmitt, B., See, C., Smith, P., Soderblom, L., Thomas, N., West, R., 2005. Rain, winds and haze during the Huygens probe's descent to Titan's surface. Nature 438, 765–778.

Wadge, G., Lopes, R.M.C., 1991. The lobes of lava flows on Earth and Olympus Mons, Mars. Bull. Volcanol. 54, 10–24.

Yung, Y.L., Allen, M., Pinto, J.P., 1984. Photochemistry of the atmosphere of Titan: Comparison between model and observations. Astrophys. J. Suppl. Ser. 55, 465–506.